Kinematics of Serial Manipulators

Ashitava Ghosal *

Abstract

This article deals with the kinematics of serial manipulators. The serial manipulators are assumed to be rigid and are modeled using the well-known Denavit-Hartenberg parameters. Two well-known problems in serial manipulator kinematics, namely the direct and inverse problems, are discussed and several examples are presented. The important concept of the workspace of a serial manipulator and the approaches to determine the workspace are also discussed.

Keywords: Serial manipulators, direct kinematics, inverse kinematics, workspace, general 6R manipulator, redundant manipulators

1 Introduction

A serial manipulator consists of a fixed base, a series of links connected by joints, and ending at a free end carrying the tool or the end-effector. In contrast to parallel manipulators, there are no closed loops. By actuating the joints, one can position and orient the end-effector in a plane or in three-dimensional (3D) space to perform desired tasks with the end-effector. This chapter deals with kinematics of serial manipulators where the motion of links are studied without considering the external forces and torques which cause these motions. The serial manipulator geometries are described using the well-known Denavit-Hartenberg (D-H) parameters. Two well-known problems, namely the *direct* and *inverse* kinematics problems, are posed, their solution procedures discussed in detail and illustrated with examples of planar and spatial serial manipulators. It is shown that closed-form analytic solutions to the inverse kinematics problem is possible only for serial manipulators with special geometries and the most general six-degree-of-freedom serial manipulator requires the solution of at most a 16th degree polynomial. The solution of the inverse kinematics problem leads to an important and useful concept of the *workspace* of a serial manipulator and the approaches to obtain the workspace and determine its properties are also presented.

As mentioned above, a serial manipulator consists of joints and links. The number of joints and links determine the *degree of freedom* of a manipulator which determines the capabilities of a serial manipulator. We start this chapter with a discussion on this important concept of degrees of freedom of a serial manipulator.

*Department of Mechanical Engineering, Indian Institute of Science, Bangalore, India. Email: asitava@mecheng.iisc.ernet.in

2 Degrees of freedom of a manipulator

The degrees of freedom of a serial manipulator[1] can be obtained from the well-known Chebychev-Grübler-Kutzbach criterion

$$\text{dof} = \lambda(N - J - 1) + \sum_{i=1}^{J} F_i \tag{1}$$

where dof is the computed degree of freedom with N as the total number of links including the fixed link (or base), J as the total number of joints connecting two consecutive links, F_i as the degrees of freedom at the i^{th} joint, and

$$\lambda = \begin{cases} 6, & \text{for motion in 3D} \\ 3, & \text{for planar motion.} \end{cases}$$

The quantity, dof, obtained from equation (1) is the number of independent actuators that can be present in the serial manipulator. In a broad sense, dof determines the capability of the serial manipulator with respect to dimension of the ambient space λ. We have the following possibilities:

1. dof $= \lambda$ – In this case, an end-effector of a manipulator can be positioned and oriented arbitrarily in the ambient space of motion.

2. dof $< \lambda$ – In this case, the arbitrary position and orientation of the end-effector is not achievable and there exist $(\lambda - \text{dof})$ functional relationships containing the position and orientation variables of the end-effector.

3. dof $> \lambda$ – These are called redundant manipulators and the end-effector can be positioned and oriented in infinite number of ways.

In serial manipulators with a fixed base, a free end-effector and two links connected by a joint, from equation (1), $N = J + 1$ and dof $= \sum_{i=1}^{J} F_i$. If all the actuated joints are one- degree-of-freedom joints, then $J = \text{dof}$.

If $J <$ dof, then one or more of the actuated joints are multi- degree-of-freedom joints and this is not used in mechanical serial manipulators. This is due to the fact that it is difficult to locate and actuate two or more one- degree-of-freedom joints at the same place in a serial manipulator. In biological systems, muscles are used to actuate multi- degree-of-freedom joints – in a human arm muscles actuate the three- degree-of-freedom shoulder joint.

In manipulators, the J joint variables form the *joint space*. The variables describing the position and orientation of a link or the end-effector are called the *task* space variables. The dimension of task space is ≤ 6 for 3D motions and ≤ 3 for planar motion. Finally, there are often mechanical linkages, gears, etc. between actuators and joints. The space of all actuator variables is called the *actuator* space. If the dimension of the actuator space is more than 3 for planar motion and more than 6 for 3D motion, the manipulator is called redundant. If the dimension of the actuator space is less than the degree of freedom, then the manipulator is called *under-actuated*.

[1]The Chebychev-Grübler-Kutzbach criterion can be used to find the degree of freedom of an arbitrary connections of links and joints and is not restricted to serial manipulators. It, however, does not work for *over-constrained* mechanisms. More details can be found in Gogu [1].

3 Representation of links using Denavit-Hartenberg parameters and transformation matrix

As mentioned earlier, the serial manipulator consists of a sequence of links connected by joints. In most industrial manipulators, the links are designed to minimize deflection and consequent loss of accuracy and repeatability, and, in this sense, the links can be assumed to be *rigid* bodies. It is well-known that a rigid body in 3D space can be described (with respect to another rigid body or a reference coordinate system) completely by six independent parameters – three for the position vector of a point of interest on the link or the origin of a coordinate system attached to the rigid body and three angles for the orientation of the rigid body. In 1955, Denavit and Hartenberg [2], presented a formulation for describing links connected by rotary (R) or prismatic (P) joints which required only four independent parameters and thus leading to more efficient computations. Unfortunately, over time, several conventions have emerged with slightly different interpretations of these four Denavit-Hartenberg or D-H parameters (see, for example textbooks by Paul [3], Fu et al. [4] and Craig [5]). In this Chapter we follow one of the commonly used and modern convention described in Craig [5] or Ghosal [6].

Figure 1 shows three rotary (R) joints connecting link $i-2$ and link $i-1$, link $i-1$ and link i and link i and link $i+1$, respectively – although R joints are used in the developement here, analogous definitions of D-H parameters with prismatic (P) joints and a sequence containing both R and P joints can be similarly obtained. The key elements of the convention used here are

- the joint axis i is labeled as $\hat{\mathbf{Z}}_i$,
- the coordinate system $\{i\}$ is attached to the link i, and
- the origin O_i of $\{i\}$ lies on the joint axis i.

It may be noted that the link i is *after*[2] the joint i as shown schematically in figure 1. The $\hat{\mathbf{X}}_i$ axis is along the mutual perpendicular between the lines along $\hat{\mathbf{Z}}_i$ and $\hat{\mathbf{Z}}_{i+1}$ and the intersection of the mutual perpendicular line and the line along joint axis i determines the origin O_i of coordinate system $\{i\}$. The $\hat{\mathbf{Y}}_i$ axis, perpendicular to both $\hat{\mathbf{X}}_i$ and $\hat{\mathbf{Z}}_i$ so as to form a right-handed coordinate system, is not shown for clarity.

The first D-H parameter for link i is the *twist angle*, α_{i-1}, defined as the angle between the lines along $\hat{\mathbf{Z}}_{i-1}$ and $\hat{\mathbf{Z}}_i$ and measured about the common perpendicular $\hat{\mathbf{X}}_{i-1}$ according to the right-hand rule (see figure 1). The twist angle is a signed quantity between 0 and $\pm\pi$ radians.

The second D-H parameter for link i is the *link length*, a_{i-1}, defined as the distance between the lines along $\hat{\mathbf{Z}}_{i-1}$ and $\hat{\mathbf{Z}}_i$ along the common perpendicular $\hat{\mathbf{X}}_{i-1}$ (see figure 1). It is a positive quantity or zero.

The third D-H parameter is called the *link offset*, d_i, defined as the displacement along $\hat{\mathbf{Z}}_i$ from the line parallel to $\hat{\mathbf{X}}_{i-1}$ to the line parallel to $\hat{\mathbf{X}}_i$. If the joint i is rotary, then d_i is a constant and for a prismatic joint d_i is the *joint variable* (see figure 1). The quantity d_i can be positive, negative or zero.

The fourth D-H parameter is the link *rotation angle*, θ_i, defined to be the angle between $\hat{\mathbf{X}}_{i-1}$ and $\hat{\mathbf{X}}_i$ measured about $\hat{\mathbf{Z}}_i$ according to the right-hand rule. If the joint i is prismatic, then θ_i is

[2]In serial manipulators, the notion of *after* is clear and natural – the fixed link is denoted by {0} and link 1, denoted {1}, is after the joint 1 connecting {0} and {1}. In parallel and hybrid manipulators, with one or more loops, one needs to be careful since the loop can be traversed in more than one way.

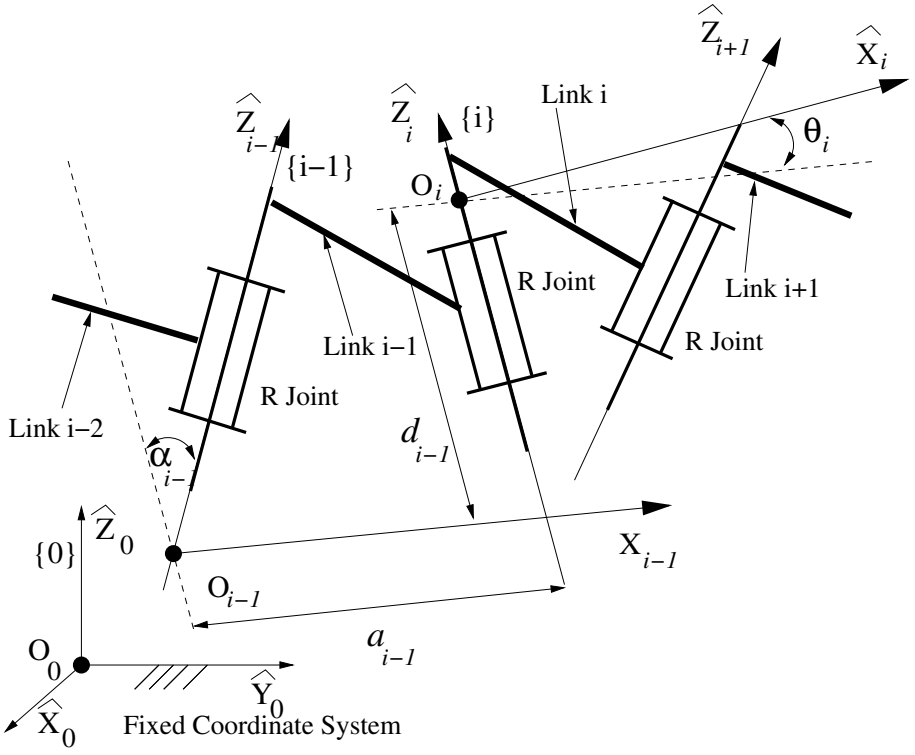

Figure 1: Intermediate links and D-H parameters

constant and if joint i is rotary, then θ_i is the *joint variable* (see figure 1). The rotation angle θ_i is a signed quantity between 0 and $\pm\pi$ radians.

If the axes of two consecutive joints $i-1$ and i are parallel, then there exists infinitely many common perpendiculars. In this case the twist angle α_{i-1} is 0 or π and the link length a_{i-1} is the distance along any of the common perpendiculars since all are equal. If the joints $i-1$ and i are parallel and the joint i is rotary, then d_i is taken as zero. If the joint i is prismatic, then θ_i is taken as zero. It may be noted that if the two consecutive joints are prismatic and parallel, then the two joint variables are not independent.

If two consecutive joints are intersecting, then there are two choices for the direction of the common perpendicular $\hat{\mathbf{X}}_{i-1}$ either along or opposite to the normal to the plane defined by the intersecting $\hat{\mathbf{Z}}_{i-1}$ and $\hat{\mathbf{Z}}_i$. The link length a_{i-1} is clearly zero.

The above assignment of origins and co-ordinate axes fails for the first and the last link. For the first link, the choice of $\hat{\mathbf{Z}}_0$ and thereby $\hat{\mathbf{X}}_1$ is arbitrary, and for the last link, $\hat{\mathbf{Z}}_{n+1}$ does not exist. As a consequence, α_{i-1} and a_{i-1} for first link and d_i and θ_i for the last link are not defined. In order to overcome this problem, the following is used:

- For the first link, if the first joint is rotary (R), then $\{0\}$ and $\{1\}$ are chosen to be coincident with $\alpha_{i-1} = a_{i-1} = 0$. This also implies $d_1 = 0$ if first joint is rotary and the only non-zero variable is θ_1.

- For the first link, if the first joint is prismatic (P), then the coordinate axes of $\{0\}$ and $\{1\}$

are chosen to be parallel and $\alpha_{i-1} = a_{i-1} = \theta_1 = 0$. For the first link with a prismatic joint, the only non-zero parameter is d_1.

- For the last (n) link, if the joint n is rotary (R), then the origins of $\{n\}$ and $\{n+1\}$ are chosen to be coincident and $d_n = 0$. The angle θ_n is taken to be zero when the axis $\hat{\mathbf{X}}_{n-1}$ aligns with axis $\hat{\mathbf{X}}_n$. The joint variable in this case is θ_n.
- If the last joint is prismatic, $\hat{\mathbf{X}}_n$ is chosen so that $\theta_n = 0$, and the origin O_n is chosen at the intersection of $\hat{\mathbf{X}}_{n-1}$ and $\hat{\mathbf{Z}}_n$ when $d_n = 0$. The joint variable in this case is d_n.

In the above described convention, two of the four parameters of the link i, α_{i-1} and a_{i-1}, have subscripts $i-1$ and two of them, d_i and θ_i, have subscript i. Another consequence of the convention is that the link length a_n and the twist angle, α_n, need not be defined. The link n is the end-effector or the tool of the manipulator and, to represent the tool or the end-effector, a separate coordinate system $\{Tool\}$ on the tool is used. Usually, this end-effector or tool coordinate system has the same orientation as $\{n\}$ and its origin is at some point of interest in $\{Tool\}$. For example, in the case of a parallel jaw gripper schematically shown in figure 2, the origin of $\{Tool\}$ is at the mid-point of the jaws.

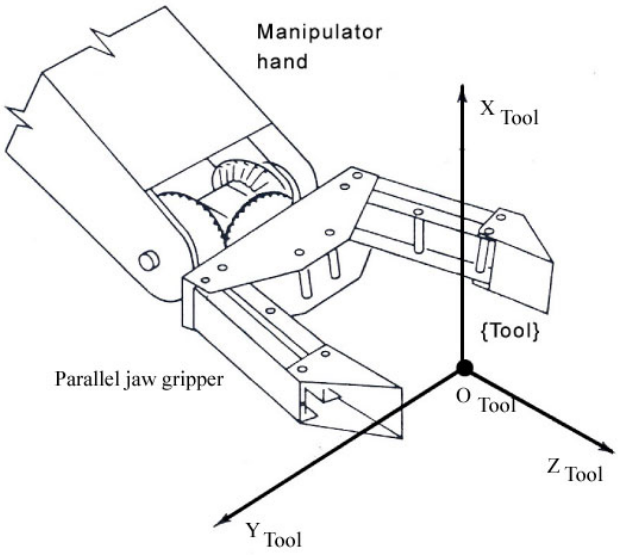

Figure 2: Parallel jaw gripper with $\{Tool\}$ frame

Once the links of a serial robot are represented with the Denavit-Hartenberg parameters, the position and orientation of link i can be obtained with respect to link $i-1$. The position vector to the origin of link i, O_i, from the origin of link $i-1$, O_{i-1}, is given by

$$^{i-1}\mathbf{O}_i = a_{i-1}\ {}^{i-1}\hat{\mathbf{X}}_{i-1} + d_i\ {}^{i-1}\hat{\mathbf{Z}}_i \tag{2}$$

where ${}^{i-1}\hat{\mathbf{X}}_{i-1}$ is $(1,0,0)^T$ and ${}^{i-1}\hat{\mathbf{Z}}_i$ is given by $(0,\ -s_{\alpha_{i-1}},\ c_{\alpha_{i-1}})^T$. It may be noted that throughout this article sine and cosine of an angle θ are denoted by s_θ, c_θ, respectively.

The rotation matrix, ${}_{i}^{i-1}[R]$, describing the orientation of link i with respect to link $i-1$, is given by the product of two rotation matrices, namely rotation of angle α_{i-1} about $\hat{\mathbf{X}}$ and rotation of angle θ_i about $\hat{\mathbf{Z}}$

$$\begin{aligned} {}_{i}^{i-1}[R] &= [R(\hat{\mathbf{X}}_{i-1}, \alpha_{i-1})]\ [R(\hat{\mathbf{Z}}_i, \theta_i)] \\ &= \begin{pmatrix} 1 & 0 & 0 \\ 0 & c_{\alpha_{i-1}} & -s_{\alpha_{i-1}} \\ 0 & s_{\alpha_{i-1}} & c_{\alpha_{i-1}} \end{pmatrix} \begin{pmatrix} c_{\theta_i} & -s_{\theta_i} & 0 \\ s_{\theta_i} & c_{\theta_i} & 0 \\ 0 & 0 & 1 \end{pmatrix} \end{aligned} \tag{3}$$

In terms of the commonly used 4×4 homogeneous transformations, the link i with respect to $i-1$ is given by

$${}_{i}^{i-1}[T] = \begin{pmatrix} c_{\theta_i} & -s_{\theta_i} & 0 & a_{i-1} \\ s_{\theta_i} c_{\alpha_{i-1}} & c_{\theta_i} c_{\alpha_{i-1}} & -s_{\alpha_{i-1}} & -s_{\alpha_{i-1}} d_i \\ s_{\theta_i} s_{\alpha_{i-1}} & c_{\theta_i} s_{\alpha_{i-1}} & c_{\alpha_{i-1}} & c_{\alpha_{i-1}} d_i \\ 0 & 0 & 0 & 1 \end{pmatrix} \tag{4}$$

It can be seen that ${}_{i}^{i-1}[T]$ is a function of *only one* joint variable – a function of θ_i if joint i is rotary and a function of d_i if joint i is prismatic.

To obtain the transformation matrix of a link i with respect to any other link, product of transformation matrices can be used. For example, the link i can be described with respect to the fixed base or reference coordinate system $\{0\}$ as

$${}_{i}^{0}[T] = {}_{1}^{0}[T]\ {}_{2}^{1}[T]\ \ldots\ {}_{i}^{i-1}[T] \tag{5}$$

Since each of ${}_{i}^{i-1}[T]$ is a function of only one joint variable, the right-hand side of equation (5) will be a function of i joint variables with the other $3*i$ Denavit-Hartenberg parameters being constant.

3.1 Examples of D-H parameters and link transformation matrices

To illustrate the concept of Denavit-Hartenberg parameters and link transformation matrices, three examples are presented in this section.

The planar 3R manipulator

As a first example, the D-H parameters and link transformation matrices of a simple planar three link manipulator with three rotary (R) joints, shown in figure 3, is obtained.

In this example, all the rotary joint axes are parallel and are pointing out of the paper. The Denavit-Hartenberg parameters are obtained as follows.

The fixed or reference coordinate system, $\{0\}$, is chosen with its $\hat{\mathbf{Z}}_0$ coming out of the paper, and $\hat{\mathbf{X}}_0$ and $\hat{\mathbf{Y}}_0$ pointing to the right and top, respectively. For the first coordinate system, the origin O_1 and $\hat{\mathbf{Z}}_1$ are coincident with O_0 and $\hat{\mathbf{Z}}_0$, and $\hat{\mathbf{X}}_1$ and $\hat{\mathbf{Y}}_1$ are coincident with $\hat{\mathbf{X}}_0$ and $\hat{\mathbf{Y}}_0$ when θ_1 is zero. The $\hat{\mathbf{X}}_1$ is along the mutual perpendicular between $\hat{\mathbf{Z}}_1$ and $\hat{\mathbf{Z}}_2$. Similarly, $\hat{\mathbf{X}}_2$ is along the mutual perpendicular between $\hat{\mathbf{Z}}_2$ and $\hat{\mathbf{Z}}_3$. For the last frame, $\hat{\mathbf{X}}_3$ is aligned to $\hat{\mathbf{X}}_2$ when $\theta_3 = 0$. The origin O_2 is located at the intersection of the mutual perpendicular along $\hat{\mathbf{X}}_2$ and $\hat{\mathbf{Z}}_2$. The origin O_3 is chosen such that d_3 is zero. The origins and the axes of $\{1\}$, $\{2\}$, and $\{3\}$ are as shown in figure 3.

From the assigned origins and axes, the Denavit-Hartenberg parameters can be obtained by inspection. They are presented in a tabular form below.

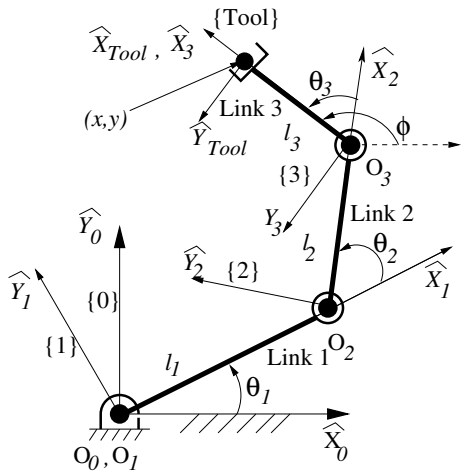

Figure 3: The planar 3R manipulator

Table 1: The D-H parameters of a planar 3R manipulator

i	α_{i-1}	a_{i-1}	d_i	θ_i
1	0	0	0	θ_1
2	0	l_1	0	θ_2
3	0	l_2	0	θ_3

In the above table, l_1 and l_2 are the link lengths as shown in figure 3. It may be noted that the length of the end-effector does not appear in the table. To describe the end-effector, we attach a tool frame, $\{Tool\}$, aligned to $\{3\}$ at the mid-point of the parallel jaw gripper. In figure 3, the origin of $\{Tool\}$ is shown at a distance of l_3 from O_3 along $\hat{\mathbf{X}}_3$.

From the D-H table, using equation (4), the link transformation matrices can be obtained by substitution. For $i = 1$, $a_{i-1} = 0$, $\alpha_{i-1} = 0$ and $d_i = 0$. Denoting $\sin\theta_1$ and $\cos\theta_1$ by s_1 and c_1, respectively, one can get

$$ {}^{0}_{1}[T] = \begin{pmatrix} c_1 & -s_1 & 0 & 0 \\ s_1 & c_1 & 0 & 0 \\ 0 & 0 & 1 & 0 \\ 0 & 0 & 0 & 1 \end{pmatrix} $$

Similarly, for $i = 2$ ($a_{i-1} = l_1$, $\alpha_{i-1} = 0$ and $d_i = 0$) and for $i = 3$ ($a_{i-1} = l_2$, $\alpha_{i-1} = 0$ and $d_i = 0$),

$$ {}^{1}_{2}[T] = \begin{pmatrix} c_2 & -s_2 & 0 & l_1 \\ s_2 & c_2 & 0 & 0 \\ 0 & 0 & 1 & 0 \\ 0 & 0 & 0 & 1 \end{pmatrix}, \qquad {}^{2}_{3}[T] = \begin{pmatrix} c_3 & -s_3 & 0 & l_2 \\ s_3 & c_3 & 0 & 0 \\ 0 & 0 & 1 & 0 \\ 0 & 0 & 0 & 1 \end{pmatrix} $$

To find the transformation matrix ${}^{3}_{Tool}[T]$, the orientation of $\{Tool\}$ is assumed to be the same as the orientation of $\{3\}$ and the origin is at a distance l_3 along $\hat{\mathbf{X}}_3$. Hence

$${}^{3}_{Tool}[T] = \begin{pmatrix} 1 & 0 & 0 & l_3 \\ 0 & 1 & 0 & 0 \\ 0 & 0 & 1 & 0 \\ 0 & 0 & 0 & 1 \end{pmatrix}$$

To find the transformation matrix ${}^{0}_{3}[T]$, multiply ${}^{0}_{1}[T]\ {}^{1}_{2}[T]\ {}^{2}_{3}[T]$ resulting in

$${}^{0}_{3}[T] = \begin{pmatrix} c_{123} & -s_{123} & 0 & l_1c_1 + l_2c_{12} \\ s_{123} & c_{123} & 0 & l_1s_1 + l_2s_{12} \\ 0 & 0 & 1 & 0 \\ 0 & 0 & 0 & 1 \end{pmatrix} \tag{6}$$

Finally, to obtain ${}^{0}_{Tool}[T]$, multiply ${}^{0}_{3}[T]\ {}^{3}_{Tool}[T]$ and get

$${}^{0}_{Tool}[T] = \begin{pmatrix} c_{123} & -s_{123} & 0 & l_1c_1 + l_2c_{12} + l_3c_{123} \\ s_{123} & c_{123} & 0 & l_1s_1 + l_2s_{12} + l_3s_{123} \\ 0 & 0 & 1 & 0 \\ 0 & 0 & 0 & 1 \end{pmatrix} \tag{7}$$

The PUMA 560 manipulator

The PUMA 560 is a six- degree-of-freedom manipulator with all rotary (R) joints. A schematic drawing of the manipulator is shown in figure 4 with the assigned coordinate systems to the links of the manipulator.

The coordinate systems $\{0\}$, $\{1\}$, and $\{2\}$ have the same origin. In many industrial manipulators, the last three joint axes intersect at a point called the "wrist" and the PUMA 560 is one such example. The origins of the coordinate systems $\{4\}$, $\{5\}$ and $\{6\}$ are located at this wrist point. Once the origins and the coordinate systems are assigned, the Denavit-Hartenberg parameters can be obtained by inspecting figure 4 and they are presented in a tabular form below.

The link transformation matrices relating successive coordinate systems can be obtained by using equation (4).

$${}^{0}_{1}[T] = \begin{pmatrix} c_1 & -s_1 & 0 & 0 \\ s_1 & c_1 & 0 & 0 \\ 0 & 0 & 1 & 0 \\ 0 & 0 & 0 & 1 \end{pmatrix}, \qquad {}^{1}_{2}[T] = \begin{pmatrix} c_2 & -s_2 & 0 & 0 \\ 0 & 0 & 1 & 0 \\ -s_2 & -c_2 & 0 & 0 \\ 0 & 0 & 0 & 1 \end{pmatrix}$$

$${}^{2}_{3}[T] = \begin{pmatrix} c_3 & -s_3 & 0 & a_2 \\ s_3 & c_3 & 0 & 0 \\ 0 & 0 & 1 & d_3 \\ 0 & 0 & 0 & 1 \end{pmatrix}, \qquad {}^{3}_{4}[T] = \begin{pmatrix} c_4 & -s_4 & 0 & a_3 \\ 0 & 0 & 1 & d_4 \\ -s_4 & -c_4 & 0 & 0 \\ 0 & 0 & 0 & 1 \end{pmatrix}$$

$${}^{4}_{5}[T] = \begin{pmatrix} c_5 & -s_5 & 0 & 0 \\ 0 & 0 & -1 & 0 \\ s_5 & c_5 & 0 & 0 \\ 0 & 0 & 0 & 1 \end{pmatrix}, \qquad {}^{5}_{6}[T] = \begin{pmatrix} c_6 & -s_6 & 0 & 0 \\ 0 & 0 & 1 & 0 \\ -s_6 & -c_6 & 0 & 0 \\ 0 & 0 & 0 & 1 \end{pmatrix}$$

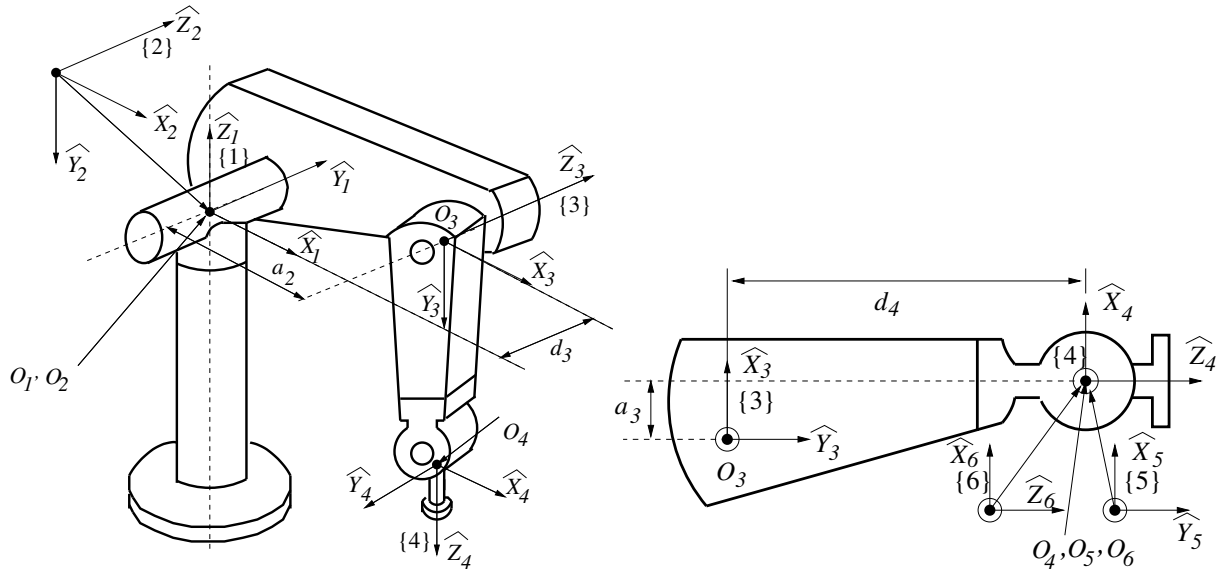

(a) The PUMA 560 manipulator

(b) Puma 560 – forearm and wrist

Figure 4: Schematic of a PUMA 560 manipulator

The transformation matrix ${}^0_6[T]$ can be obtained by multiplying all the above transformation matrices. The matrix ${}^0_3[T]$ is obtained by multiplying ${}^0_1[T]$ ${}^1_2[T]$ ${}^2_3[T]$ and is given by

$$ {}^0_3[T] = \begin{pmatrix} c_1c_{23} & -c_1s_{23} & -s_1 & a_2c_1c_2 - d_3s_1 \\ s_1c_{23} & -s_1s_{23} & c_1 & a_2s_1c_2 + d_3c_1 \\ -s_{23} & -c_{23} & 0 & -a_2s_2 \\ 0 & 0 & 0 & 1 \end{pmatrix} \tag{8} $$

The matrix ${}^3_6[T]$ is obtained by multiplying ${}^3_4[T]$ ${}^4_5[T]$ ${}^5_6[T]$.

$$ {}^3_6[T] = \begin{pmatrix} c_4c_5c_6 - s_4s_6 & -c_4c_5s_6 - s_4c_6 & -c_4s_5 & a_3 \\ s_5c_6 & -s_5s_6 & c_5 & d_4 \\ -s_4c_5c_6 - c_4s_6 & s_4c_5s_6 - c_4c_6 & s_4s_5 & 0 \\ 0 & 0 & 0 & 1 \end{pmatrix} \tag{9} $$

The transformation matrix ${}^0_6[T]$ can be obtained by multiplying ${}^0_3[T]$ and ${}^3_6[T]$ given in equations (8) and (9).

A SCARA manipulator

A manipulator with a SCARA configuration is very popular for robotic assembly due to its compliance and rigidity in desired directions. A SCARA manipulator has four degrees of freedom with three rotary (R) joints and the third joint is prismatic (P). Figure 5 shows a schematic drawing of a SCARA manipulator and the assigned coordinate systems.

As shown in the figure 5, the coordinate systems {0} and {1} have the same origin and the origins of {3} and {4} are chosen at the base of the parallel jaw gripper. The directions of $\hat{\mathbf{Z}}_3$

Table 2: The D-H parameters of a PUMA 560 manipulator

i	α_{i-1}	a_{i-1}	d_i	θ_i
1	0	0	0	θ_1
2	$-\pi/2$	0	0	θ_2
3	0	a_2	d_3	θ_3
4	$-\pi/2$	a_3	d_4	θ_4
5	$\pi/2$	0	0	θ_5
6	$-\pi/2$	0	0	θ_6

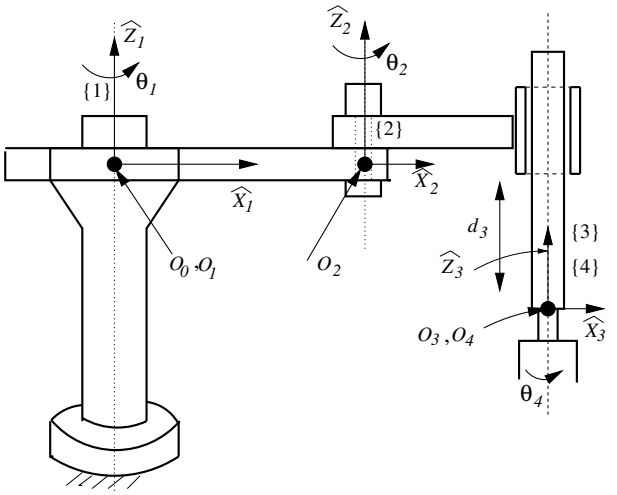

Figure 5: A SCARA manipulator

have been as chosen pointing upwards. It may be noted that the $\hat{\mathbf{Z}}_3$ can be chosen in the opposite direction and O_3 can be chosen at some other point – the kinematic properties of the SCARA manipulator will not chnage but d_3 values will be different. In an actual SCARA manipulator, the translation at the third joint may be realized by means of a (rotary) motor and a ball-screw. However, in this example, the third joint is assumed to be a prismatic (P) joint.

The Denavit-Hartenberg parameters can now be obtained by inspecting figure 6 and they are presented in a tabular form below.

The link transformation matrices relating successive links or coordinate systems can be obtained by using equation (4) and are given below.

$$ {}^{0}_{1}[T] = \begin{pmatrix} c_1 & -s_1 & 0 & 0 \\ s_1 & c_1 & 0 & 0 \\ 0 & 0 & 1 & 0 \\ 0 & 0 & 0 & 1 \end{pmatrix}, \qquad {}^{1}_{2}[T] = \begin{pmatrix} c_2 & -s_2 & 0 & a_1 \\ s_2 & c_2 & 0 & 0 \\ 0 & 0 & 1 & 0 \\ 0 & 0 & 0 & 1 \end{pmatrix} $$

Table 3: The D-H parameters of a SCARA manipulator

i	α_{i-1}	a_{i-1}	d_i	θ_i
1	0	0	0	θ_1
2	0	a_1	0	θ_2
3	0	a_2	$-d_3$	0
4	0	0	0	θ_4

$$ {}^{2}_{3}[T] = \begin{pmatrix} 1 & 0 & 0 & a_2 \\ 0 & 1 & 0 & 0 \\ 0 & 0 & 1 & -d_3 \\ 0 & 0 & 0 & 1 \end{pmatrix}, \qquad {}^{3}_{4}[T] = \begin{pmatrix} c_4 & -s_4 & 0 & 0 \\ s_4 & c_4 & 0 & 0 \\ 0 & 0 & 1 & 0 \\ 0 & 0 & 0 & 1 \end{pmatrix} $$

The transformation matrix ${}^{0}_{4}[T]$ is obtained as

$$ \begin{aligned} {}^{0}_{4}[T] &= {}^{0}_{1}[T]\ {}^{1}_{2}[T]\ {}^{2}_{3}[T]\ {}^{3}_{4}[T] \\ &= \begin{pmatrix} c_{124} & -s_{124} & 0 & a_1c_1 + a_2c_{12} \\ s_{124} & c_{124} & 0 & a_1s_1 + a_2s_{12} \\ 0 & 0 & 1 & -d_3 \\ 0 & 0 & 0 & 1 \end{pmatrix} \end{aligned} \tag{10} $$

In the next section one of the main problems in serial manipulator kinematics is posed and discussed in detail.

4 Direct kinematics of serial manipulators

The direct kinematics problem of a serial manipulator can be stated as follows: given the link parameters and the joint variable, a_{i-1}, α_{i-1}, d_i, and θ_i, find the position and orientation of the last link in the fixed or reference coordinate system.

The direct kinematics is the simplest possible problem in manipulator kinematics and it follows directly from the notion of the link transformation matrix of Section 3. If the fixed coordinate system is $\{0\}$ and the coordinate system of the end-effector is $\{n\}$, one can write

$$ {}^{0}_{n}[T] = {}^{0}_{1}[T]{}^{1}_{2}[T].....{}^{n-1}_{n}[T] \tag{11} $$

In the above matrix equation, the right-hand side contains a_{i-1}, α_{i-1}, d_i, θ_i with $1 = 1, ..., n$. In the direct kinematics problem, all these are known and hence all the 4×4 matrices on the right-hand side are known. The direct kinematics problem for serial manipulators can thus be solved by simple matrix multiplication and extraction of the rotation matrix, ${}^{0}_{n}[R]$, and the vector to the origin, ${}^{0}\mathbf{O}_n$, of $\{n\}$.

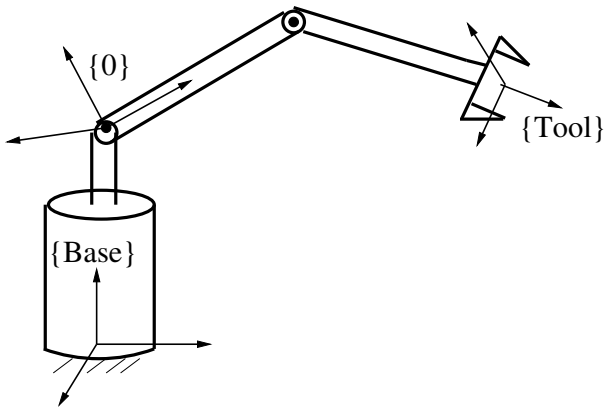

Figure 6: The $\{Base\}$ and $\{Tool\}$ frames

Instead of orientation and position of ${}^{0}_{n}[T]$, it is often of interest to obtain ${}^{Base}_{n}[T]$ (see figure 6). To obtain ${}^{Base}_{n}[T]$, pre-multiply ${}^{0}_{n}[T]$ by a known ${}^{Base}_{0}[T]$. Likewise to obtain ${}^{Tool}_{0}[T]$, post-multiply ${}^{0}_{n}[T]$ by a known ${}^{n}_{Tool}[T]$. In general,

$$ {}^{Base}_{Tool}[T] = {}^{Base}_{0}[T] \; {}^{0}_{n}[T] \; {}^{n}_{Tool}[T] \tag{12} $$

One of the advantages of the D-H convention used here is that manipulator kinematics, represented by ${}^{0}_{n}[T]$, is *independent* of the choise of the $\{Base\}$ or the $\{Tool\}$, and very little change is required if the serial robot changes its end-effector or is moved to some other location on the factory floor. This feature is not available in several of the other conventions in use for defining D-H parameters.

The direct kinematics problems for three serial manipulators are solved in the following examples.

4.1 Example – The planar 3R manipulator

In the case of the planar 3R manipulator (see figure 3), the orientation of the tool or the gripper can be described by an angle ϕ. From equation (7), one can directly write the position coordinates, x, y, and orientation of the tool as

$$ \begin{aligned} x &= l_1 c_1 + l_2 c_{12} + l_3 c_{123} \\ y &= l_1 s_1 + l_2 s_{12} + l_3 s_{123} \\ \phi &= \theta_1 + \theta_2 + \theta_3 \end{aligned} \tag{13} $$

where, c_{12}, s_{12} etc. represent $\cos(\theta_1 + \theta_2)$ and $\sin(\theta_1 + \theta_2)$ etc., respectively.

4.2 Example – The PUMA 560 manipulator

The transformation matrix ${}^{0}_{6}[T]$ for the PUMA manipulator is obtained by multiplying ${}^{0}_{3}[T]$ and ${}^{3}_{6}[T]$ given in equations (8) and (9). Denoting the elements of the rotation matrix ${}^{0}_{6}[R]$ by $r_{ij},\ i,j = 1,2,3,$

and the components of the origin of the coordinate system $\{6\}$, ${}^0\mathbf{O}_6$, by $(O_{6x}, O_{6y}, O_{6z})^T$, one can write

$$\begin{aligned}
r_{11} &= c_1\{c_{23}(c_4c_5c_6 - s_4s_6) - s_{23}s_5c_6\} + s_1(s_4c_5c_6 + c_4s_6) \\
r_{21} &= s_1\{c_{23}(c_4c_5c_6 - s_4s_6) - s_{23}s_5c_6\} - c_1(s_4c_5c_6 + c_4s_6) \\
r_{31} &= -s_{23}(c_4c_5c_6 - s_4s_6) - c_{23}s_5c_6 \\
\\
r_{12} &= c_1\{c_{23}(-c_4c_5s_6 - s_4c_6) + s_{23}s_5s_6\} + s_1(-s_4c_5s_6 + c_4c_6) \\
r_{22} &= s_1\{c_{23}(-c_4c_5s_6 - s_4c_6) + s_{23}s_5s_6\} - c_1(-s_4c_5s_6 + c_4c_6) \\
r_{32} &= -s_{23}(c_4c_5s_6 - s_4c_6) + c_{23}s_5s_6 \\
\\
r_{13} &= -c_1(c_{23}c_4s_5 + s_{23}c_5) - s_1s_4s_5 \\
r_{23} &= -s_1(c_{23}c_4s_5 + s_{23}c_5) + c_1s_4s_5 \\
r_{33} &= s_{23}c_4s_5 - c_{23}c_5 \\
\\
O_{6x} &= c_1(a_2c_2 + a_3c_{23} - d_4s_{23}) - d_3s_1 \\
O_{6y} &= s_1(a_2c_2 + a_3c_{23} - d_4s_{23}) + d_3c_1 \\
O_{6z} &= -a_2s_2 - a_3s_{23} - d_4c_{23}
\end{aligned} \tag{14}$$

4.3 Example – A SCARA manipulator

For the SCARA manipulator, the matrix ${}^0_4[T]$ is given in equation (10). The orientation of the $\{4\}$ can be described by the angle ϕ, and the position, (x, y, z) of origin of $\{4\}$ is given by

$$\begin{aligned}
x &= a_1c_1 + a_2c_{12} \\
y &= a_1s_1 + a_2s_{12} \\
z &= -d_3 \\
\phi &= \theta_1 + \theta_2 + \theta_4
\end{aligned} \tag{15}$$

It may be noted that the direct kinematics problem for a serial manipulator is *well defined*, *easily solvable*, and has a *unique solution* for any number of links.

5 Inverse kinematics of serial manipulators

The inverse kinematics problem for serial manipulators can be stated as follows: given the constant link parameters and the position and orientation of $\{n\}$ with respect to the fixed frame $\{0\}$, find the joint variables. For the planar 3R manipulator example, the inverse kinematics problem would be to obtain $\theta_i,\ i = 1, 2, 3$, given the position of the end-effector x, y and its orientation ϕ. In the case of the spatial PUMA manipulator, the transformation matrix ${}^0_6[T]$ is given and the goal is to find the joint angles $\theta_i,\ i = 1, .., 6$. In general, six task space variables are given for 3D motion (three task space variables for planar motion) and the goal is to find the n joint variables which make up ${}^0_n[T]$. Depending on n, the following cases are possible:

Case 1: $n = 6$ for motion in 3D or $n = 3$ for a planar motion. In this case, there exists required number of equations for the unknowns.

Case 2: $n < 6$ for motion in 3D or $n < 3$ for a planar motion. In this case, the number of task space variables is more than the number of equations and hence, for solutions to exist, there must be $6 - n$ ($3 - n$ for planar case) relationships involving the task space variables.

Case 3: $n > 6$ for motion in 3D or $n > 3$ for a planar motion. In this case there are more unknowns than equations and hence there exists infinite number of solutions. These are called redundant manipulators.

5.1 Inverse kinematics for Case 1

It can be seen from the direct kinematics equations of the planar 3R or the spatial PUMA manipulator (see equations (13) and (14)), the position and orientation of the end-effector are related to the joint variables by means of *non-linear transcendental* equations. In order to solve the inverse kinematics problem, one needs to solve these non-linear equations. Ideally, the goal is to obtain *closed-form* and *analytical* expressions for the joint variables in terms of the given position and orientation of the last link. Like most sets of non-linear equations, no known general methods for solving the inverse kinematics problem for an arbitrary serial manipulator was available till the work of Raghavan and Roth [7]. Before looking at this general method, to obtain insight, it is useful to solve the inverse kinematics for a few simple serial manipulators.

Example – The planar 3R manipulator

For the planar 3R manipulator shown in figure 3, the direct kinematics equations are given in equation (13). To solve for $\theta_i,\ i = 1, 2, 3$, given $x,\ y,\ \phi$, one can proceed as follows:

Define $X = x - l_3 c_\phi$ and $Y = y - l_3 s_\phi$ X and Y are known. Squaring and adding, one can get

$$X^2 + Y^2 = l_1^2 + l_2^2 + 2 l_1 l_2 c_2$$

and one can get

$$\theta_2 = \pm \cos^{-1}\left(\frac{X^2 + Y^2 - l_1^2 - l_2^2}{2 l_1 l_2}\right) \tag{16}$$

Once θ_2 is known, θ_1 can be found using the four quadrant arc tangent formula as

$$\theta_1 = \text{Atan2}(Y, X) - \text{Atan2}(k_2, k_1) \tag{17}$$

where $k_2 = l_2 s_2$ and $k_1 = l_1 + l_2 c_2$. Finally, θ_3 can be obtained from

$$\theta_3 = \phi - \theta_1 - \theta_2 \tag{18}$$

The *workspace* of the planar 3R manipulator is defined as the set of values of $\{x, y, \phi\}$ for which the inverse kinematics solution *exists*. The workspace for the planar 3R manipulator can be obtained by examining equation (16). It is known that

$$-1 \leq \left(\frac{X^2 + Y^2 - l_1^2 - l_2^2}{2 l_1 l_2}\right) \leq +1$$

which implies that

$$(l_1 - l_2)^2 \leq (X^2 + Y^2) \leq (l_1 + l_2)^2 \tag{19}$$

where $X = x - l_3 c_\phi$ and $Y = y - l_3 s_\phi$. Figure 7 shows a 3D plot of the region in $\{x, y, \phi\}$ space where the inequalities in equation (19) are satisfied and the inverse kinematics solution *exists*. A

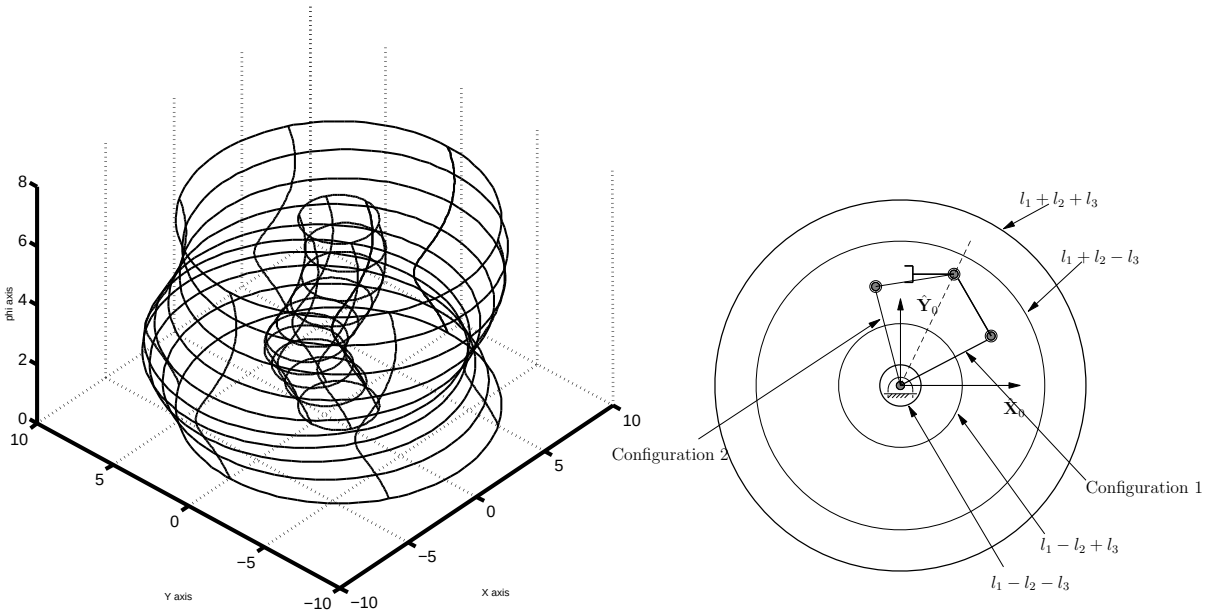

(a) 3D workspace of 3R manipulator

(b) $X - Y$ projection of workspace of 3R manipulator

Figure 7: Workspace of a planar 3R robot

projection of the workspace on the $\hat{X}_0 - \hat{Y}_0$ plane is shown in figure 7 for $l_1 > l_2 > l_3$. We have four circles of radius $l_1 + l_2 + l_3$, $l_1 + l_2 - l_3$, $l_1 - l_2 + l_3$ and $l_1 - l_2 - l_3$.

It can be seen from figure 7 that the maximum reach of the planar 3R manipulator are points on the circle of radius $l_1 + l_2 + l_3$ and the closest it can reach from the origin are points on the circle of radius $l_1 - l_2 - l_3$. This annular region is called the *reachable* workspace. Points in-between the other two circles of radii $l_1 + l_2 - l_3$ and $l_1 - l_2 + l_3$ can be reached with *any* ϕ and this region was named as *dexterous* workspace by Kumar and Waldron [8, 9]. It can be seen that as l_3 increases, the reachable workspace increases whereas the dexterous workspace decreases.

Given any point in the workspace, the inverse kinematics procedure gives two sets of values of θ_1, θ_2, and θ_3. This is shown schematically in figure 7 – the given X and Y can be reached by the two configurations. As with any non-linear equation, the solutions are non-unique and one could have several solutions. In the planar 3R manipulator, one can have *two sets* of solutions.

Example – The PUMA 560 manipulator

For the six- degree-of-freedom PUMA 560 manipulator shown in figure 4, the direct kinematics equations are given in equation (14). In the PUMA 560 manipulator, the last three axes intersect at a "wrist" point. Due to this geometry, the position of the origin of the last link ($\{6\}$) is only a function of joint variables θ_1, θ_2, and θ_3. Denoting the coordinates of the wrist point by $(x, y, z)^T$, one can write,

$$\begin{aligned} x &= c_1(a_2c_2 + a_3c_{23} - d_4s_{23}) - d_3s_1 \\ y &= s_1(a_2c_2 + a_3c_{23} - d_4s_{23}) + d_3c_1 \\ z &= -a_2s_2 - a_3s_{23} - d_4c_{23} \end{aligned} \tag{20}$$

From the first two equations, one can write

$$-s_1 x + c_1 y = d_3$$

The above transcendental equation can be solved for θ_1 by making the well-known tangent half-angle substitution

$$\begin{aligned} x_1 &= \tan\frac{\theta_1}{2} \\ \cos\theta_1 &= \frac{1-x_1^2}{1+x_1^2}, \quad \sin\theta_1 = \frac{2x_1}{1+x_1^2} \end{aligned} \tag{21}$$

which *converts* the transcendental equation to the quadratic

$$x_1^2(d_3 + y) + 2xx_1 + (d_3 - y) = 0$$

The above quadratic can be solved in closed form for x_1 and one can obtain

$$\theta_1 = 2\tan^{-1}\left(\frac{-x \pm \sqrt{x^2 + y^2 - d_3^2}}{y + d_3}\right) \tag{22}$$

It may be noted that $\tan^{-1}$ gives an angle between 0 and π and hence $0 \leq \theta_1 \leq 2\pi$. However, due to the $\pm$ sign before the square root, there are two possible values of θ_1.

To obtain θ_3 observe that

$$x^2 + y^2 + z^2 = d_3^2 + a_2^2 + a_3^2 + d_4^3 + 2a_2a_3c_3 - 2a_2d_4s_3$$

which involves only sine and cosine of θ_3. Again using tangent half-angle substitutions one can get

$$\theta_3 = 2\tan^{-1}\left(\frac{-d_4 \pm \sqrt{d_4^2 + a_3^2 - K^2}}{K + a_3}\right) \tag{23}$$

where the constant K is given as $(1/2a_2)(x^2 + y^2 + z^2 - d_3^2 - a_2^2 - a_3^2 - d_4^2)$. Again, $\tan^{-1}$ gives an angle between 0 and π and hence $0 \leq \theta_3 \leq 2\pi$. Due to the $\pm$ sign, one can get two possible values of θ_3.

Finally, to obtain an expression for θ_2, observe that the Z component of the wrist point is only a function of θ_2 and θ_3. The third equation in (20) can be written as

$$-s_2(a_2 + a_3c_3 - d_4s_3) + c_2(-a_3s_3 - d_4c_3) = z$$

and one can obtain

$$\theta_2 = 2\tan^{-1}\left(\frac{-a_2 - a_3c_3 + d_4s_3 \pm \sqrt{a_2^2 + a_3^2 + d_4^2 + 2a_2(a_3c_3 - d_4s_3) - z^2}}{z - (a_3s_3 + d_4c_3)}\right) \tag{24}$$

Again $0 \leq \theta_2 \leq 2\pi$ and there exists two possible values of θ_2 due to the $\pm$ sign. Since θ_3 appears on the right-hand side of equation (24) in c_3 and s_3 and one can have two possible values of θ_3, there exists four possible values of θ_2.

The last three joint angles θ_4, θ_5 and θ_6 can be obtained from ${}^3_6[R]$ given by

$${}^3_6[R] = \begin{pmatrix} c_4c_5c_6 - s_4s_6 & -c_4c_5s_6 - s_4c_6 & -c_4s_5 \\ s_5c_6 & -s_5s_6 & c_5 \\ -s_4c_5c_6 - c_4s_6 & s_4c_5s_6 - c_4c_6 & s_4s_5 \end{pmatrix}$$

One can also write

$${}^3_6[R] = {}^0_3[R]^T {}^0_6[R]$$

and since θ_1, θ_2, and θ_3 are now known, the right-hand side is known. Let the right-hand side matrix elements be denoted by r_{ij}, $i, j = 1, 2, 3$. The following algorithm can be used to obtain θ_4, θ_5, and θ_6.

Algorithm $r_{ij} \Rightarrow \theta_4$**,** θ_5 **and** θ_6
If $r_{23} \neq \pm 1$, *then*
$\theta_5 = \text{Atan2}(\pm\sqrt{(r_{21}^2 + r_{22}^2)}, r_{23})$
$\theta_4 = \text{Atan2}(r_{33}/s_5, -r_{13}/s_5)$,
$\theta_6 = \text{Atan2}(-r_{22}/s_5, r_{21}/s_5)$
Else
If $r_{23} = 1$, *then*
$\theta_4 = 0$
$\theta_5 = 0$,
$\theta_6 = \text{Atan2}(-r_{12}, r_{11})$,
If $r_{23} = -1$, *then*
$\theta_4 = 0$
$\theta_5 = \pi$,
$\theta_6 = -\text{Atan2}(r_{12}, -r_{11})$,

The inverse kinematics of a PUMA 560 gives rise to two values of θ_1, two values of θ_3, four values of θ_2, i.e., there exists 4 sets of values of $(\theta_1, \theta_2, \theta_3)$ for a given wrist location. The above algorithm gives two sets of values for $(\theta_4, \theta_5, \theta_6)$ for each set of $(\theta_1, \theta_2, \theta_3)$. Hence a PUMA 560 manipulator can have at most *eight* possible configurations.

The workspace of a PUMA 560 manipulator is the set of values of the position and orientation of the last link, n, for which the inverse kinematics solution exists. It is not possible to imagine or describe the workspace since it is a six dimensional entity. One can, however, obtain the reachable workspace of the wrist point. The position vector of the wrist point is given in equation (20) and the set of all (x, y, z) satisfying equation (20) is a *solid* in 3D space. The bounding surface(s) of the solid can be obtained as follows:
Squaring and adding the three equations in equation (20) and simplifying, one can get

$$R^2 = x^2 + y^2 + z^2 = K_1 + K_2c_3 - K_3s_3$$

where K_1, K_2, and K_3 are constants. The envelope of this family of surfaces satisfies

$$\frac{\partial R^2}{\partial \theta_3} = 0$$

which gives

$$K_2s_3 + K_3c_3 = 0$$

Eliminating θ_3 from these two equations, and denoting $a_3^2 + d_4^2$ by l^2, one can get,

$$[x^2 + y^2 + z^2 - ((a_2 + l)^2 + d_3^2)][x^2 + y^2 + z^2 - ((a_2 - l)^2 + d_3^2)] = 0 \tag{25}$$

The above shows that the bounding surfaces for the wrist point are spheres.

The orientation workspace for a PUMA 560 are like a set of three Euler angles about *two* distinct axes. In particular, they are the so-called $Z - Y - Z$ rotations except that the second Y rotation is $-\theta_5$. As it is well-known, except for two special 'singular' configurations, the three Euler angles can be obtained for any arbitrary rotation matrix. Hence, at every point in the 3D solid, the last link can be oriented arbitrarily except at the two 'wrist singular' configurations.

Numerical example of a PUMA 560

For the PUMA 560, the numerical values of the constant Denavit-Hartenberg parameters and the ranges of the joint variables are given by

i	α_{i-1}	a_{i-1}	d_i	Range of θ_i
	degrees	m	m	degrees
1	0	0	0	$-160 \leq \theta_1 \leq 160$
2	-90	0	0	$-245 \leq \theta_2 \leq 45$
3	0	0.4318	0.1245	$-45 \leq \theta_3 \leq 225$
4	-90	0.0203	0.4318	$-110 \leq \theta_4 \leq 170$
5	90	0	0	$-100 \leq \theta_5 \leq 100$
6	-90	0	0	$-266 \leq \theta_6 \leq 266$

For an arbitrarily chosen $\theta_1 = 90$, $\theta_2 = 30$, $\theta_3 = 60$, $\theta_4 = 135$, $\theta_5 = -60$ and $\theta_6 = 120$, the transformation matrix ${}^0_6[T]$ is obtained as

$${}^0_6[T] = \begin{bmatrix} -0.7891 & 0.0474 & 0.6124 & -0.1245 \\ -0.4330 & -0.7500 & -0.5000 & -0.0579 \\ 0.4356 & -0.6597 & 0.6214 & -0.2362 \\ 0 & 0 & 0 & 1 \end{bmatrix} \tag{26}$$

The above ${}^0_6[T]$ can be used as an input to the inverse kinematics algorithm. Using the inverse kinematics equations, eight sets of solutions are obtained as

i	θ_1	θ_2	θ_3	θ_4	θ_5	θ_6
1	139.85	2.48	60.00	-0.80	65.29	-122.53
2	139.85	2.48	60.00	179.20	-65.29	57.47
3	90.00	30.00	60.00	-45.00	60.00	-60.00
4	90.00	30.00	60.00	135.00	-60.00	120.00
5	139.85	150.00	125.38	-178.64	147.61	58.28
6	139.85	150.00	125.38	1.36	-147.61	-121.72
7	90.00	177.52	125.38	-111.60	138.80	155.68
8	90.00	177.52	125.38	68.40	-138.80	-24.32

As expected, one of the solutions (set 4) matches the chosen values of θ_i, $i = 1, ..., 6$, in the direct kinematics.

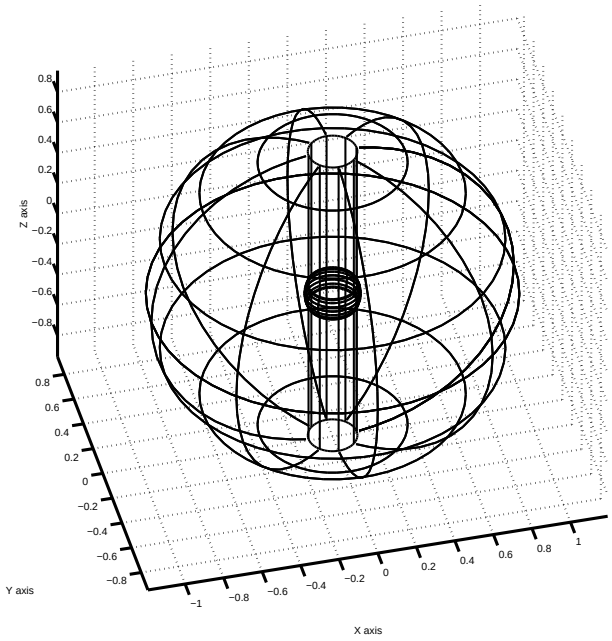

Figure 8: Workspace of the wrist point of the PUMA 560

The workspace of the wrist point of the PUMA 560 for the numerical values assumed in this example is shown in figure 8. It may be noted that the *actual* workspace of the PUMA 560 robot is only a subset due to the presence of joint limits.

In above two examples, and in general for **Case 1**, analytical solution of the inverse kinematics problem requires the elimination of joint variables from sets of non-linear transcendental equations to finally arrive at a single equation in one joint variable which can then be solved. When three consecutive joint axis intersect (PUMA 560 is such an example) instead of dealing with non-linear equations containing all six joint variables, the inverse kinematics problem can be decomposed into two problems each involving only three equations in three joint variables [10]. This decoupling was first noticed by Pieper [11] who worked on the well-known Stanford Arm. It was later shown that when three consecutive joint axis intersect, one needs to solve at most a fourth-order polynomial in the tangent of a joint angle, and the manipulator wrist point can reach any position in the 3D workspace in at most four possible ways. Since fourth-degree polynomials can be solved in closed form (see p. 24 in Korn and Korn [12]), the inverse kinematics of all six- degree-of-freedom serial manipulators with three intersecting axes can be solved in closed form.

For the PUMA 560, the workspace of the wrist point is bounded by two spheres. This is due to the fact that the PUMA has a special geometry. In a general serial robot with three joint axis intersecting at a wrist, it can be shown that the boundaries of the solid region traced by the wrist point form a torus which is a fourth-degree surface [13]. Typically, it is not a complete torus since the joints cannot rotate fully and some points on the torus and inside cannot be reached. The effect of joint limits on the workspace has been studied by several authors (see, for example, [14, 15]).

For serial manipulators where three consecutive joint axis do not intersect, the elimination procedure to solve the inverse kinematics problem is much more complex. Several researchers

worked on this problem – Duffy and Crane [16] first derived a 32^{nd} order polynomial and it was finally demonstrated by Raghavan and Roth [7] that the inverse kinematics of an arbitrary 6R serial manipulator required the solution of at most a sixteenth-degree polynomial. Alternately, the inverse kinematics of any serial manipulator can also be solved *numerically* and this is illustrated for a serial robot where only the last two joint axis intersect.

Manipulator with non-intersecting wrist

The three axes intersecting wrist, as in the PUMA 560 manipulator, is a fairly complicated design and also difficult to manufacture. In addition, there is always some manufacturing tolerance that makes it impossible to have three axes intersecting exactly at a point. Consider a robot similar to the PUMA 560 but with a non-zero offset d_5 which makes the last three joint axis non-intersecting. For such a robot, the last column of ${}^0_6[T]$ can be written as

$$\begin{aligned} x &= c_1(a_2c_2 + a_3c_{23} - d_4s_{23}) - d_3s_1 + d_5(s_1c_4 - c_1s_4c_{23}) \\ y &= s_1(a_2c_2 + a_3c_{23} - d_4s_{23}) + d_3c_1 - d_5(c_1c_4 + s_1s_4c_{23}) \\ z &= -a_2s_2 - a_3s_{23} - d_4c_{23} - d_5s_4s_{23} \end{aligned} \tag{27}$$

Equations (27) are in four joint variables $(\theta_1, \theta_2, \theta_3, \theta_4)$ in terms of known x, y, and z. To solve for the unknown joint variable, one additional equation is required containing the same joint variables. The additional equation, in this example, can be obtained by examining the rotation matrices. Since the inverse of a rotation matrix is the same as its transpose,

$${}^3_6[R] = {}^0_3[R]^T {}^0_6[R]$$

where ${}^0_6[R]$ have known elements $r_{ij},\ i,j = 1,2,3$. The above equation can be expanded to obtain

$$\begin{pmatrix} c_4c_5c_6 - s_4s_6 & -c_4c_5s_6 - s_4c_6 & -c_4s_5 \\ s_5c_6 & -s_5s_6 & c_5 \\ -s_4c_5c_6 - c_4s_6 & s_4c_5s_6 - c_4c_6 & s_4s_5 \end{pmatrix} = \begin{pmatrix} c_1c_{23} & s_1c_{23} & -s_{23} \\ -c_1s_{23} & -s_1s_{23} & -c_{23} \\ -s_1 & c_1 & 0 \end{pmatrix} \begin{pmatrix} r_{11} & r_{12} & r_{13} \\ r_{21} & r_{22} & r_{23} \\ r_{31} & r_{32} & r_{33} \end{pmatrix} \tag{28}$$

From the $(1,3)$ and $(3,3)$ terms of the above matrix equation, for $\theta_5 \neq 0, \pi$, one can get

$$s_4(r_{13}c_1c_{23} + r_{23}s_1c_{23} - r_{33}s_{23}) = c_4(r_{13}s_1 - r_{23}c_1) \tag{29}$$

Equations (27) and (29) can be solved for $(\theta_1, \theta_2, \theta_3, \theta_4)$ by using any available numerical scheme. Using the D-H parameter values for the PUMA 560, $d_5 = 20$ mm, the ${}^0_6[T]$ given in equation (26) and using the numerical solver *fsolve* in Matlab [17], one can obtain

$$\theta_1 = 96.11,\ \theta_2 = 169.11, \theta_3 = 128.93, \theta_4 = -115.51$$

Once $(\theta_1, \theta_2, \theta_3)$ are obtained, θ_4, θ_5, and θ_6 can be solved by considering left- and right-hand sides of the matrix equation (28). For $\theta_5 \neq 0, \pi$,

$$\begin{aligned} \theta_5 &= \text{Atan2}(\pm\sqrt{(1,3)^2 + (3,3)^2}, (2,3)) \\ \theta_4 &= \text{Atan2}((3,3)/s_5, -(3,1)/s_5) \\ \theta_6 &= \text{Atan2}(-(2,2)/s_5, (2,1)/s_5) \end{aligned}$$

where the terms $(3,3)$, $(2,2)$, etc. are from the right-hand side of equation (28) and are known once θ_1, θ_2, and θ_3 are known. For the numerical values chosen above, two sets of values, namely, $\theta_4 = -115.51, 64.49$, $\theta_5 = 141.99, -141.99$, and $\theta_6 = 146.54, -33.46$ are obtained. It can be verified that one value of θ_4 is the same as the value obtained using *fsolve*. It may be noted that $\theta_5 = 0$ or π is a *singular* configuration for the non-intersecting wrist.

Efficient numerical techniques, such as the Newton-Raphson method using available Jacobian matrices of serial manipulators (see Chapter on velocity analysis), can solve the inverse kinematics problem of a serial manipulator extremely quickly in very few iterations (typically 2 or 3). The two main issues associated with any numerical technique are the choice of the initial guess and effort required to find *all* solutions. In practice, the choice of the initial guess is not serious since the initial guess can be the previous values of the joint variables[3]. The second difficulty is not easily overcome even though continuation methods [18] can be used to obtain all the solutions. Analytical expressions have the advantage of finding *all* possible inverse kinematics solutions and also give insight into the nature of the workspace. This has been a motivating reason for finding general algorithms for the inverse kinematics of arbitrary serial manipulators.

Inverse kinematics of a general 6R robot

As mentioned earlier, in the 1990's Raghavan and Roth [7] developed a general algorithm to solve the inverse kinematics of an arbitrary 6R serial manipulator. The manipulator is arbitrary in the sense that none of the fixed Denavit-Hartenberg parameters (link lengths, twist angles, or link offsets) have special values, such as 0, $\pi/2$, or π, which results in simpler equations and easier elimination of one or more joint variables. The salient features of the algorithm are presented next.

For a general 6R serial manipulator, the direct kinematics equations can be written as

$$ {}^0_6[T] = {}^0_1[T]{}^1_2[T]{}^2_3[T]{}^3_4[T]{}^4_5[T]{}^5_6[T] \tag{30} $$

where ${}^{i-1}_i[T]$ is in terms of the four Denavit-Hartenberg parameters and is a function of only one joint variable θ_i (or d_i) and the other three Denavit-Hartenberg parameters are constants (see equation (4)). For the inverse kinematics problem, the left-hand side ${}^0_6[T]$ is given and the six joint variables in each of ${}^{i-1}_i[T]$, $i = 1, 2, ..., 6$ are to be obtained.

The first step is to recognize that ${}^{i-1}_i[T]$ can be written as a product of two 4×4 matrices, $({}^{i-1}_i[T])_{st}({}^{i-1}_i[T])_{jt}$. The first matrix $({}^{i-1}_i[T])_{st}$ is a function of a_{i-1} and α_{i-1} and is constant and the second matrix $({}^{i-1}_i[T])_{jt}$ is a function of the joint variables θ_i (for a rotary joint) or d_i (for a prismatic joint). Thus one can write

$$ \begin{aligned} {}^{i-1}_i[T] &= ({}^{i-1}_i[T])_{st}({}^{i-1}_i[T])_{jt} \\ &= \begin{pmatrix} 1 & 0 & 0 & a_{i-1} \\ 0 & c_{\alpha_{i-1}} & -s_{\alpha_{i-1}} & 0 \\ 0 & s_{\alpha_{i-1}} & c_{\alpha_{i-1}} & 0 \\ 0 & 0 & 0 & 1 \end{pmatrix} \begin{pmatrix} c_{\theta_i} & -s_{\theta_i} & 0 & 0 \\ s_{\theta_i} & c_{\theta_i} & 0 & 0 \\ 0 & 0 & 1 & d_i \\ 0 & 0 & 0 & 1 \end{pmatrix} \end{aligned} \tag{31} $$

[3]For accurate control, a manipulator end-effector is commanded to move by a small amount from its present position and orientation. The joint values at the future commanded position and orientation are expected to be close to the known current values and these current values of the joint variables serve as a very good initial guess for the numerical procedure.

The second step is to rewrite equation (30) as

$$({}^{2}_{3}[T])_{jt}\ {}^{3}_{4}[T]{}^{4}_{5}[T]({}^{5}_{6}[T])_{st} = ({}^{2}_{3}[T])^{-1}_{st}\ ({}^{1}_{2}[T])^{-1}({}^{0}_{1}[T])^{-1}\ {}^{0}_{6}[T]({}^{5}_{6}[T])^{-1}_{jt} \tag{32}$$

It maybe seen that the left-hand side is only a function of $(\theta_3, \theta_4, \theta_5)$ and the right-hand side is only a function of $(\theta_1, \theta_2, \theta_6)$. In addition, it can be found that in the six scalar equations obtained by equating the top three elements of columns 3 and 4 on both sides of equation (32) do not contain θ_6. Denoting the third and fourth columns by $\mathbf{p}$ and $\mathbf{l}$, one can rewrite the six equations as

$$[A](s_4s_5\ \ s_4c_5\ \ c_4s_5\ \ c_4c_5\ \ s_4\ \ c_4\ \ s_5\ \ c_5\ \ 1)^T = [B](s_1s_2\ \ s_1c_2\ \ c_1s_2\ \ c_1c_2\ \ s_1\ \ c_1\ \ s_2\ \ c_2)^T \tag{33}$$

where $[A]$ is 6×9 matrix whose elements are linear in s_3, c_3, 1, and $[B]$ is 6×8 matrix of constants.

The third step is to eliminate four of the five variables, θ_1, θ_2, θ_3, θ_4, and θ_5 in equation (33). As pointed out by Raghavan and Roth [7], the minimal set of equations are 14 in number. These are the three equations from $\mathbf{p}$, three equations from $\mathbf{l}$, one scalar equation from the scalar dot product $\mathbf{p} \cdot \mathbf{p}$, one scalar equation from the scalar dot product $\mathbf{p} \cdot \mathbf{l}$, three equations from the vector cross product $\mathbf{p} \times \mathbf{l}$, and three scalar equations from $(\mathbf{p} \cdot \mathbf{p})\mathbf{l} - (2\mathbf{p} \cdot \mathbf{l})\mathbf{p}$. It is shown that all these 14 equations contain the same variables as in equation (33) with no new variables. The 14 equations can be written as

$$[P]\,(s_4s_5\ \ s_4c_5\ \ c_4s_5\ \ c_4c_5\ \ s_4\ \ c_4\ \ s_5\ \ c_5\ \ 1)^T = [Q]\,(s_1s_2\ \ s_1c_2\ \ c_1s_2\ \ c_1c_2\ \ s_1\ \ c_1\ \ s_2\ \ c_2)^T \tag{34}$$

where $[P]$ is a 14×9 matrix whose elements are linear in c_3, s_3, 1, and $[Q]$ is a 14×8 matrix of constants. To eliminate four out of the five joint rotations, use any eight of the 14 equations in equation (34) and solve for the eight variables $s_1s_2, s_1c_2, c_1s_2, c_1c_2, s_1, c_1, s_2, c_2$. Note, this is always possible since this involves solving eight linear equations in eight unknowns. Once this is done, substitute the eight variables in the rest of the six equations and get an equation of the form

$$[R]\,(s_4s_5\ \ s_4c_5\ \ c_4s_5\ \ c_4c_5\ \ s_4\ \ c_4\ \ s_5\ \ c_5\ \ 1)^T = \mathbf{0} \tag{35}$$

where $[R]$ is a 6×9 matrix whose elements are linear in s_3 and c_3.

In the fourth step, the tangent half-angle formulas (see equation (21)) are introduced for s_3, c_3, s_4, c_4, s_5, c_5, and after simplification, obtain

$$[S]\,\left(x_4^2x_5^2\ \ x_4^2x_5\ \ x_4^2\ \ x_4x_5^2\ \ x_4x_5\ \ x_4\ \ x_5^2\ \ x_5\ \ 1\right)^T = \mathbf{0} \tag{36}$$

where $[S]$ is a 6×9 matrix and $x_{(\cdot)} = \tan(\theta_{(\cdot)}/2)$.

In the fifth step, x_4 and x_5 are eliminated using Sylvester's dialytic method (for a treatment of elimination of variables from a set of non-linear equation, see references Salmon [19] and Raghavan and Roth [20]). Six additional equations are generated by multiplying equations in equation (36) by x_4. In the process, three additional 'linearly' independent variables, namely, $x_4^3x_5^2$, $x_4^3x_5$, and x_4^3, are generated, and a system of 12 equations in 12 unknowns are obtained. The equations can be written as

$$\begin{pmatrix} S & 0 \\ 0 & S \end{pmatrix} \left(x_4^3x_5^2\ \ x_4^3x_5\ \ x_4^3\ \ x_4^2x_5^2\ \ x_4^2x_5\ \ x_4^2\ \ x_4x_5^2\ \ x_4x_5\ \ x_4\ \ x_5^2\ \ x_5\ \ 1\right)^T = \mathbf{0} \tag{37}$$

Following Sylvester's dialytic method, the determinant of the coefficient matrix is set to zero and this gives a 16th-degree polynomial in x_3. The roots of this polynomial can be solved numerically

and then one can find $\theta_3 = 2\tan^{-1}(x_3)$. Since there can be 16 real solutions to the polynomial, the general 6R serial manipulator has 16 possible configurations.

In the final step from known θ_3, x_4 and x_5 (and θ_4, θ_5) are obtained from equation (37) using standard tools of linear algebra. Once θ_3, θ_4, and θ_5 are known, using equation (36), the right-hand side variables s_1s_2, s_1c_2, ..., s_2, c_2 are solved from the eight linearly independent equations and thus unique θ_1 and θ_2 are obtained. Finally, to obtain θ_6, equation (30) is rewritten as

$$ {}^5_6[T] = {}^4_5[T]^{-1}\,{}^3_4[T]^{-1}\,{}^2_3[T]^{-1}\,{}^1_2[T]^{-1}\,{}^0_1[T]^{-1}\,{}^0_6[T] \tag{38} $$

Since $\theta_i, i = 1, 2, ..., 5$ are known, the $(1, 1)$ and $(2, 1)$ element gives two equations in s_6 and c_6 which gives unique values of θ_6.

It may be noted that if the 6R manipulator has special geometry, i.e., some Denavit-Hartenberg parameters are 0, $\pi/2$, or π, the 16th-degree polynomial in x_3 can be of lower order. In addition, if one or more joints are prismatic, then the inverse kinematics problem becomes simpler since the prismatic joint variable is not in terms of sines or cosines. The 16th-degree polynomial is not amenable to analysis as in the case of a planar 3R or the PUMA 560 and it is not possible to obtain the workspace or the boundaries of a general 6R serial manipulator. However, if all the roots of the 16th-degree polynomial are complex, then ${}^0_6[T]$ is *not* in the workspace of the manipulator and this reasoning can be used to get some idea of the workspace of the general 6R serial manipulator.

Finally, in industrial applications, a choice needs to be made from the possible inverse kinematic solution sets to move the end-effector to the desired position and orientation. This is done in two steps – first, all solution sets in which atleast one joint variable is outside the joint limits is rejected. For example, out of the 8 possible solutions in the numerical example for the PUMA 560 serial manipulator, solution sets 2, 5 and 7 are not possible since the value of θ_4 is outside the joint limits of θ_4. Likewise solution sets 6, 7 and 8 have θ_5 outside its range. In the second step, out of the remaining possible inverse kinematic solutions (solutions 1, 3 and 4 for the PUMA 560), the solution set which is *closest* to the previous joint values is chosen. This strategy will not work if the solution branches come close to each other or if they intersect. Typically, path planning for a serial manipulator is done such that it is away from a singularity where the solution branches intersect.

5.2 Inverse kinematics for Case 2

In many robotic applications such as welding or painting, the rotation of the welding torch or the paint gun about its *own* axis is not required. To decrease cost and to simplify the design and manufacture, many welding or painting robots have five degrees of freedom with five actuators. Likewise, in the assembly of electronic components on a printed circuit board, it is simpler to assemble from one direction. Hence an assembly robot such as the SCARA robot has only four degrees of freedom. In these industrial robots $n < 6$, and the tool or the end-effector cannot be positioned and oriented arbitrarily in 3D space. There exists $6 - n$ ($3 - n$ for planar manipulators) relationships or constraints involving the position and orientation variables, and the given ${}^0_n[T]$ must satisfy these relationships or constraints. In most situations, the constraints are obvious since the manipulator was designed with the constraint in mind. For example, in the case of the SCARA manipulator of section 4.3, the tool can be positioned arbitrarily in 3D space but its orientation capabilities are restricted to rotations about $\hat{\mathbf{Z}}_4$ (see figure 5). Hence, the constraints would be that rotations about $\hat{\mathbf{X}}_4$ and $\hat{\mathbf{Y}}_4$ are zero. For the SCARA manipulator, given x, y, z, and ϕ, the inverse kinematics problem can be solved as

$$\begin{aligned} \theta_2 &= \pm\cos^{-1}\left(\frac{x^2+y^2-l_1^2-l_2^2}{2l_1l_2}\right) \\ \theta_1 &= \text{Atan2}(y,x) - \text{Atan2}(l_2s_2, l_1+l_2c_2) \\ d_3 &= -z \\ \theta_4 &= \phi - \theta_1 - \theta_2 \end{aligned} \tag{39}$$

The constraints or the relationships between the position and orientation variables in any serial manipulator can be, *in principle*, determined from the direct kinematics equations. For example, in a five- degree-of-freedom robot, one can obtain six equations from ${}^0_5[T]$ in terms of the five joint variables. Elimination, using Sylvester's dialytic method or any other approach, of the five joint variables from the six equations can yield a *single* equation in terms of the position and orientation variables of the tool. This single equation would be the constraint and would represent a five dimensional subspace of the reachable workspace. A manipulator with four joints would lead to two expressions involving the position and orientation variables and thus one would get four-dimensional subspace. Obtaining explicit expressions for the constraints is, however, difficult in practice due to the difficulties in elimination of variables from non-linear equations.

5.3 Inverse kinematics for Case 3

In the case of a redundant manipulator, the number of joint variables are more than the number of equations. As an illustration, consider the planar 3R serial manipulator shown in figure 3. In addition, consider that the orientation of the last link is not of interest. In such a situation, there are only two equations relating the (x, y) coordinates of the end-effector with the three joint variables, $\theta_i,\ i = 1, 2, 3$, and these are

$$\begin{aligned} x &= l_1c_1 + l_2c_{12} + l_3c_{123} \\ y &= l_1s_1 + l_2s_{12} + l_3s_{123} \end{aligned} \tag{40}$$

For the inverse kinematics, (x, y) are given and the task is to find θ_1, θ_2, and θ_3. Since there are only two equations, there exists an infinite number of solutions for θ_1, θ_2, and θ_3 for a given (x, y). In order to obtain a *finite* number of θ_1, θ_2, and θ_3, one more equation involving θ_1, θ_2, and θ_3 is needed. One can impose a simple constraint such as θ_3 equals constant (the third joint is locked), but that defeats the purpose of designing and building manipulators with more than required joints and actuators. The availability of an extra joint can be used for optimization. Several researchers have suggested the use of redundancy to minimize joint rotations, joint velocities, and accelerations. Several others have also suggested the use of redundancy for avoiding singularities and avoiding obstacles (see the textbook by Nakamura [22] and the references therein). Obtaining meaningful and useful equations is known as the *resolution* of redundancy, and this is the key issue in inverse kinematics of redundant robots. The resolution of redundancy can be achieved at various levels, such as position, velocity, accelerations, and torques. In this chapter, the example of the redundant planar 3R manipulator is used to illustrate the minimization of joint rotations – minimzation of joint velocities, accelerations and torques use the pseudo-inverse of the manipulator Jacobian matrix and this is discussed elsewhere.

A candidate function for optimization is $\theta_1^2 + \theta_2^2 + \theta_3^2$. Minimization of $\theta_1^2 + \theta_2^2 + \theta_3^2$ subject to constraints given in equation (40) results in the planar 3R manipulator following a given trajectory with least rotation of the joints and can be formulated as follows:

Minimize $f(\boldsymbol{\theta}) = \theta_1^2 + \theta_2^2 + \theta_3^2$

subject to

$$\begin{aligned} g_1(\boldsymbol{\theta}) &= -x + l_1 c_1 + l_2 c_{12} + l_3 c_{123} = 0 \\ g_2(\boldsymbol{\theta}) &= -y + l_1 s_1 + l_2 s_{12} + l_3 s_{123} = 0 \end{aligned}$$

where $\boldsymbol{\theta}$ denotes the three joint variables $(\theta_1, \theta_2, \theta_3)$, and (x, y) are points on the trajectory of the end-effector. Using the classical method of Lagrange multipliers, differentiating the modified objective function, one can get three equations

$$\begin{aligned} \frac{\partial f}{\partial \boldsymbol{\theta}} &= \lambda_1 \frac{\partial g_1}{\partial \boldsymbol{\theta}} + \lambda_2 \frac{\partial g_2}{\partial \boldsymbol{\theta}} \\ g_1(\boldsymbol{\theta}) &= 0 \\ g_2(\boldsymbol{\theta}) &= 0 \end{aligned}$$

To solve the above three equations, eliminate the Lagrange multipliers λ_1 and λ_2 by rewriting the first equation as

$$\begin{pmatrix} \frac{\partial f}{\partial \theta_1} & \frac{\partial g_1}{\partial \theta_1} & \frac{\partial g_2}{\partial \theta_1} \\ \frac{\partial f}{\partial \theta_2} & \frac{\partial g_1}{\partial \theta_2} & \frac{\partial g_2}{\partial \theta_2} \\ \frac{\partial f}{\partial \theta_3} & \frac{\partial g_1}{\partial \theta_3} & \frac{\partial g_2}{\partial \theta_3} \end{pmatrix} \begin{pmatrix} 1 \\ -\lambda_1 \\ -\lambda_2 \end{pmatrix} = 0$$

For non-trivial λ_1 and λ_2 the determinant of the 3×3 matrix must be zero and one can get, after simplification,

$$l_1 l_2 \theta_3 s_2 + l_2 l_3 (\theta_1 - \theta_2) s_3 + l_3 l_1 (\theta_3 - \theta_2) s_{23} = 0 \tag{41}$$

The inverse kinematics of the redundant planar 3R manipulator can now be solved from the three equations in (40) and (41). Figure 9 shows the plot of θ_1, θ_2, θ_3, and $f(\boldsymbol{\theta})$ (l_1, l_2, and l_3 are chosen to be 5, 3, and 1, respectively) when the end-effector of the planar 3R manipulator traces a straight line parallel to the Y axis as shown in the bottom of figure 9. One can also solve the optimization problem subject to joint limits. Figure 10 shows the plots of θ_1, θ_2, θ_3, and $f(\boldsymbol{\theta})$ when θ_2 is constrained to lie between $\pm 120^\circ$. One can observe the difference in *all* joint variables when θ_2 is constrained.

The inverse kinematics of redundant serial manipulators is an active topic of research and finds application in elephant trunk manipulators, snake robots, actuated endoscopes and various other multi-degree-of-freedom devices. The reader is refered to the references [21, 22] for the well-known pseudo-inverse based approaches, reference [23] for the modal approach and references [24, 25] for the tractrix curve based approach. The reference cited above are by no means comprehensive and there exists a vast amount of literature on redundant manipulators.

6 Conclusion

Serial manipulators are extensively used in industry for a variety of applications. A serial manipulator consists of series of links and joints connected one after another, with one end fixed and one free end carrying the tool or the end-effector. Most serial manipulators have heavy and "rigid" links and the well-known four Denavit-Hartenberg parameters can be used to mathematically represent the links and joints of a serial manipulator.

There are two important problems in serial manipulator kinematics, namely the direct and inverse kinematics problem. The direct kinematics problem involves obtaining the position and

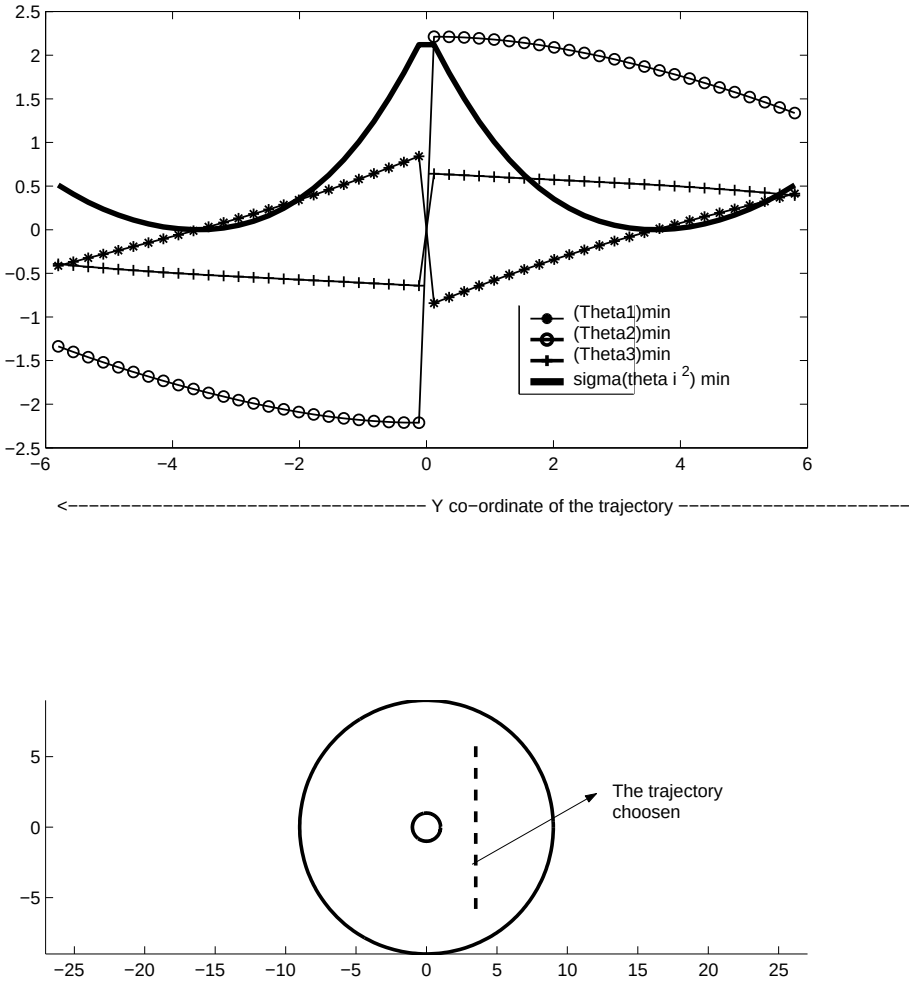

Figure 9: Plot of joint and task space variables for redundant planar 3R robot

orientation of the tool or the end-effector for given values of the joint variables. This is probably the simplest problem in robotics and can be *always* solved *uniquely* by simply multiplying appropriate matrices. The inverse kinematics problem involves obtaining joint variables for given values of the position and orientation of the tool or the end-effector and is much harder to solve. Closed-form analytic solutions can be obtained only for special geometries of the serial manipulator such as when the last three joint axis intersect at a wrist point. For such special geometries, the inverse kinematics involves solution of a fourth degree polynomial and the manipulator can reach a point in the 3D workspace in four possible ways. At each such location there can be two possible orientations. For a general six degree-of-freedom serial manipulator with arbitrary geometry, the inverse kinematics problem involves numerical solution of a 16th degree polynomial and the manipulator can reach a desired position and orientation in at most 16 possible ways. When the degree of freedom is less than 6 for spatial motion and less than 3 for planar motion, the end-effector cannot achieve arbitrary positions and orientations and there exists one or more constraints relating the position and orientation variables of the end-effector. When the number of actuated joints are more than the

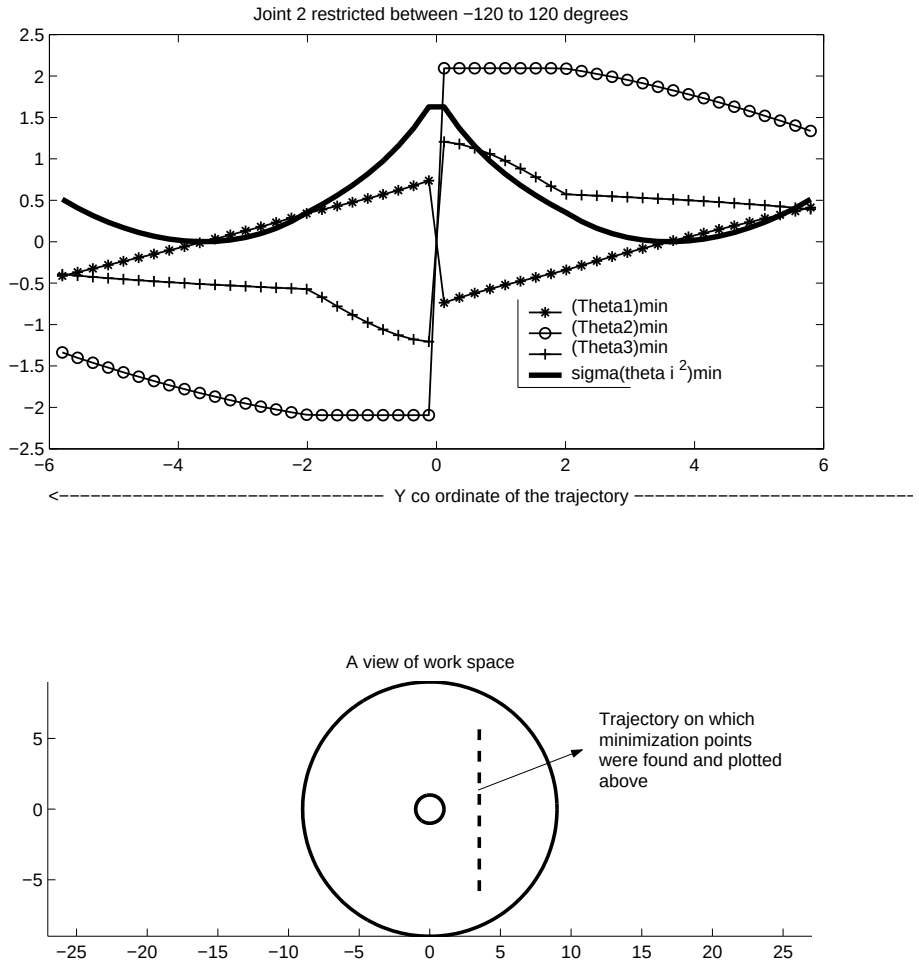

Figure 10: Plot of joint task space variables for redundant planar 3R robot with joint limit

dimension of the ambient space in which the manipulator operate, there exists an infinite number of solutions and the manipulator can reach desired position and orientation in infinite number of ways. For such redundant manipulators, optimization of a useful objective function is performed to make use of the redundancy.

The workspace of a serial manipulator is the region in 3D space which the manipulator can reach. For serial manipulators with a wrist, the workspace is a torus which is restricted when joint limits are present. The workspace of a general 6R serial manipulator cannot be described analytically. However, whether a desired position and orientation of the end-effector is achievable or not can be determined by solving the inverse kinematics problem.

Acknowledgement

The author wishes to thank his research students Ashith Shyam and Ashwin for help with numerical computations.

References

[1] Gogu G (2005) Mobility of mechanisms: a critical review. *Mechanism and Machine Theory* 40:1068-1097.

[2] Denavit J and Hartenberg R S (1955) A kinematic notation for lower-pair mechanisms based on matrices. *Trans. ASME, Journal of Applied Mechanics*, 23:215-221.

[3] Paul R (1981) *Robot Manipulators* MIT Press, Cambridge, MA.

[4] Fu K, Gonzalez R and Lee C S G (1987) *Robotics: Control, Sensing, Vision and Intelligence*, McGraw-Hill.

[5] Craig J J (2005) *Introduction to Robotics: Mechanics and Control.* 3rd Ed., Pearson Education Inc.

[6] Ghosal A (2006) *Robotics: Fundamental Concepts and Analysis*, Oxford University Press.

[7] Raghavan M and Roth B (1993) Inverse kinematics of the general 6R manipulator and related linkages. *Trans. ASME, Journal of Mechanical Design*, 115:502-508.

[8] Kumar A and Waldron K J (1980) The dexterous workspace. ASME paper no. 80-DET-108.

[9] Kumar A and Waldron K J (1981) The workspace of a mechanical manipulator. *Trans. ASME, Jou. of Mechanical Design*, 103:665-672.

[10] Paden B (1986) *Kinematics and Control of Robot Manipulators.* Ph. D. Thesis, Dept. of Mechanical Engineering, University of California, Berkeley.

[11] Pieper D L (1968) *The Kinematics of Manipulators under Computer Control.* Ph. D. Thesis, Dept. of Mechanical Engg., Stanford University.

[12] Korn G A and Korn T M (1968) *Mathematical Handbook for Scientists and Engineers.* 2nd Ed., McGraw-Hill Book Company.

[13] Tsai Y C and Soni A H (1984) The effect of link parameters on the working space of the general 3R robot arms. *Mechanisms and Machine Theory*, 19:9-16.

[14] Rastegar J and Deravi P (1987) The effect of joint motion constraints on the workspace and number of configurations of manipulators. *Mechanism and Machine Theory*, 22:401-409.

[15] Dwarakanath T A, Ghosal A and Shrinivasa U (1992) Kinematic analysis and design of articulated manipulators with joint motion constraints. *Trans. ASME, Jou. of Mechanical Design*, 116:969-972.

[16] Duffy J and Crane C (1980) A displacement analysis of the general spatial 7R mechanism. *Mechanisms and Machine Theory*, 15:153-169.

[17] Matlab (2012), *Version 7.12.0 (R2011a).* The MathWorks Inc., Natick, Massachusetts.

[18] Tsai L-W and Morgan A (1985) Solving the kinematics of the most general six- and five-degree-of-freedom manipulators by continuation methods. *Trans. ASME, Jou. of Mechanisms, Transmissions and Automation in Design*, 107:189-200.

[19] Salmon G (1964) *Lessons Introductory to Modern Higher Algebra.* Chelsea Publishing Co.

[20] Raghavan M and Roth B (1995) Solving polynomial systems for kinematic analysis and synthesis of mechanisms and robot manipulators. *Trans. ASME, Jou. of Mechanical Design*, 117:71-79.

[21] Klein C A and Huang C H (1983) Review of pseudo-inverse for control of kinematically redundant mannipulators. *IEEE Trans., Systems, Man and Cybernetics*, SMC-13:245-250.

[22] Nakamura Y (1991) *Advanced Robotics: Redundancy and Optimization*, Addison-Wesley.

[23] Chirikjian G S and Burdick J W (1994) A modal approach to hyper-redundant manipulator kinematics. *IEEE Trans. on Robotics and Automation*, 10:343-354.

[24] Reznik D and Lumelsky V (1995) Sensor-based motion planning in three dimensions for a highly redundant snake robot. *Advanced Robotics*, 9:255-280.

[25] Ravi V C, Rakshit S and Ghosal A (2010) Redundancy resolution using tractrix – simulation and experiments. *Trans. ASME, Jou. of Mechanisms and Robotics*, 2:031013-1.